The reservoir property modeling of volcanic reservoir: An application to the Shahejie Formation, Zaoyuan oilfield, eastern China

Yuming Liu[1], Rongji Zhang[2], Zhentong Xia[1], Lei Bao[1], and Jiagen Hou[1]

Abstract

As an increasing number of volcanic reservoirs has been discovered all over the world, the study of volcanic reservoirs has caught more attention. However, researchers mainly focus on the characterization of the external architecture of volcanic rock mass and the superimposed relationship between the rock mass, while paying little attention to the fine anatomy of the internal structure of the rock mass, making it difficult to effectively guide the development of the volcanic reservoir. Taking Zao35 block in Huanghua depression, Bohai Bay Basin, China, as an example, we find a workflow of establishing a high-resolution volcanic stratigraphic structure model and reservoir properties models by integrating well- and seismic-data analysis. The seismic data indicate that the volcanic activities consist of three stages: Stages I and III have positive seismic amplitude reflections, whereas stage II has a negative seismic reflection. The well data indicate that the lithology column of target formation in our study area consists of eight volcanic strata and seven mudstone strata. According to the lithology interpreted using well data, stages III, II, and I consist of five, one, and two volcanic eruption periods, respectively. We have established a structure and stratigraphy model with eight zones of volcanic rock and seven zones of mudstone barrier (15 zones in total) to effectively distinguish volcanic rocks (products of the eruption period) from sedimentary rocks (products of the volcanic dormant period). Based on the seismic attribute analysis, we have combined the sequential indicator simulation and local anisotropy from the seismic amplitude attribute. The model of volcanism can be reproduced by sequential indication simulation of local variogram with variable range directions. Based on the principle of "facies control" (perform lithology simulation in different regions according to lithofacies), we have used the sequential indication method to simulate volcanic rocks. The simulation results have a very good agreement with the shape of lava flows spreading around the crater. To describe the internal structure of the volcanic rock body, reveal internal lithology distribution characteristics, and reservoir physical properties, we provide an effective research method for the development of volcanic reservoir geologic research.

Introduction

With the development of petroleum exploration, more oil and gas reservoirs have been found in volcanic reservoirs throughout the world, and researchers gradually pay more attention to the study of volcanic reservoirs. The volcanic reservoir is one type of unconventional reservoirs, which can produce high-quality reservoir with good primary porosity (20%–35% mostly from air pore) and permeability (300–2000 mD) properties under magmatic condensation and diagenesis. Till 2016, 300 volcanic oil and gas reservoirs have been discovered in the world (Schutte, 2003; Jia et al., 2007), with proven oil reserves of more than 3.4×10^8 t and natural gas reserves of nearly 7000×10^8 m^3 (account for approximately 1% of the proven oil and gas reserves throughout the world), which fully reveals the great exploration and development potential of volcanic rocks (Jiang et al., 2010; Zhu et al., 2016).

At present, the research on volcanic rocks has extended to study volcanic lithology and lithofacies, volcanic mechanism (central eruption and fissure eruption), volcanic reservoir, volcanic reservoir modeling, and so on. The volcanic reservoir space is mainly divided into primary pores, secondary pores, and fractures (Vernik, 1990; Levin, 1995; Gamberi, 2001; Ogilvie, 2001; Schutte, 2003; Wang et al., 2011; Gu et al., 2002; Zhang et al., 2013; Huang et al., 2014). Most scholars believe that the distribution of volcanic reservoirs is mainly controlled by lithofacies, and the classification of volcanic reservoirs mainly is based on the analysis,

[1]China University of Petroleum (Beijing), State Key Laboratory of Petroleum Resources and Prospecting, Beijing, China and China University of Petroleum (Beijing), College of Geosciences, Beijing, China. E-mail: liuym@cup.edu.cn (corresponding author); xiazt96@foxmail.com; greenlantren@foxmail.com; houjg63@cup.edu.cn.

[2]China National Petroleum Corp, Dagang Oilfield, Tianjin, China. E-mail: xlk12@foxmail.com.

Manuscript received by the Editor 18 February 2021; revised manuscript received 18 January 2022; published ahead of production 28 February 2022; published online 13 April 2022. This paper appears in *Interpretation*, Vol. 10, No. 2 (May 2022); p. T351–T366, 18 FIGS.
http://dx.doi.org/10.1190/INT-2021-0048.1.

DOI:10.1190/INT-2021-0048.1

comparison, and estimation of the distribution of volcanic facies (Luo et al., 1996; Yan et al., 1996; Gao et al., 2013). The spatial distribution of volcanic rocks is predicted by analyzing the seismic attribute, such as reflection energy, frequency, and waveform (Hao et al., 2010; Cortez and Cetalte-Santos, 2016; Infante-Paez and Marfurt, 2017). Volcanism is characterized by its instantaneity and period. Volcanism originated from strong tectonic movement, and magma spewed out to the surface with multistage tectonic activity, forming periodic lava flows and volcanic debris deposits (Figure 1). According to the different volcanic conduits, scholars divided volcanic eruption into central eruption (Figure 2a), fissure eruption (Figure 2b), and compound eruption (Pike, 1978; Zangmo et al., 2016; Chen et al., 2009; Langella et al., 2009). In a central eruption, magma rises to the surface along the fixed volcanic conduits, and the effusive rocks are regularly distributed outward along the volcanic conduits. The magma of fissure eruption rises to the surface along a fault system and usually has a large distribution with few pyroclastic flows.

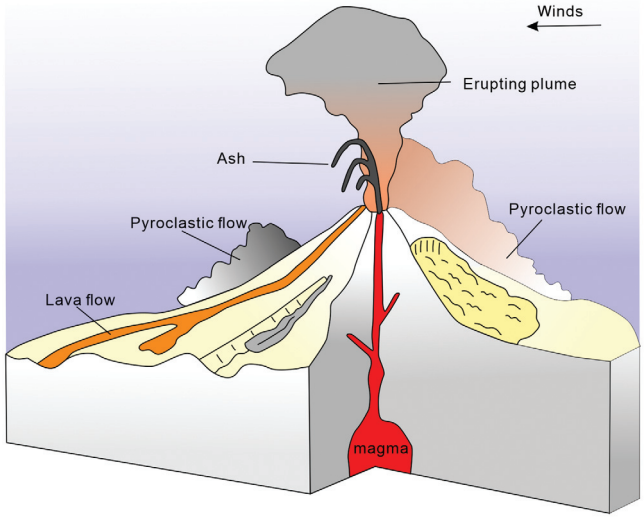

Figure 1. Volcanism is characterized by its instantaneity and period, and it urges magma up to the surface along the volcanic conduit, creating lava flow and pyroclastic flow.

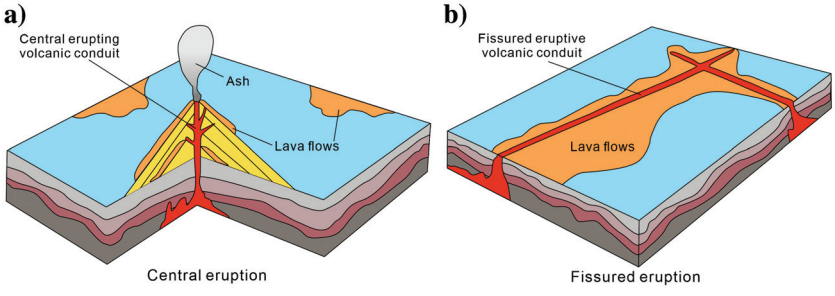

Figure 2. Typical eruption types of modern volcanoes. Central eruption has a fixed conduit and a symmetrical mound with a crater in the conduit. The fissured eruption is characterized by a large area of lava flows from the fault.

The exploration and development of volcanic reservoirs are a challenging problem, and there are few cases for reference (Wang and Zhang, 2012). At present, the exploration and development of sandstone, carbonate oil, and gas fields have entered the stage of 3D quantitative comprehensive geologic modeling of individual reservoirs. However, there are few publications about characterizing volcanic reservoirs. The geologic conditions that make it very difficult to characterize the volcanic reservoirs include multiple magma eruptions from multiple volcanic craters, the complex and variable texture of rocks, paleogeographic environment, volcanic eruption type, tectonic action, and diagenesis. Thus, it is urgent to accelerate the development and research work on the topic.

A 3D geologic modeling is not only a basic method for reservoir description and characterization but also an important means to solve the aeolotropism of the volcanic rock reservoir. Some scholars have used different seismic facies characteristics to divide volcanic rocks, and completed the geologic modeling of volcanic rocks based on "volume control" (taking the single volcanic rocks as a unit) through seismic volume constraints (Li et al., 2000; Wang, 2015; Qiu et al., 2017). Most scholars focus on the characterization of the outer contour of volcanic rock mass and the superimposed relationship between the rocks, but they paid little attention to the fine anatomy of the internal structure of the rock mass, thereby making it difficult to effectively guide the development of volcanic rock reservoirs.

Stochastic simulation technique based on geostatistics is a useful tool, which can be used to solve the distribution of volcanic rock reservoirs. There are rich stochastic simulation algorithms, such as Gaussian simulation, sequential indicator simulation, and Markov random simulation (Xia et al., 2005; Li et al., 2008; Wu et al., 2009). The sequential indicator simulation method has been used to simulate the spatial distribution of volcanic rocks, which can partly reflect the different lithology of volcanic rock lithology on the space distribution rule (Tang and Pu, 2020).

Zao35 block of Zaoyuan oilfield in Cangdong sag of Bohai Bay Basin, China, is a volcanic reservoir, with 14.25 million tons of geologic reserves (Zheng et al., 2006). Since it was put into development in 1996, Zao35 block has experienced the primary oil recovery from waterdrive and waterflood development of secondary recovery (Figure 6) (Yao et al., 2007). At present, the water production rate of oil wells is as high as 90%, but the recovery rate is only 6%, indicating low development efficiency. The main reasons affecting the development include the volcanic rock mass in the target layer has strong heterogeneity, various rock types inside the rock mass, a great difference in physical properties of different lithologies, complex vertical superposi-

DOI:10.1190/INT-2021-0048.1

tion, and rapid change in lithology periods, so to effectively predict the distribution of the reservoir becomes a challenging task.

In this paper, the Zao35 block is taken as an example to establish a high-precision volcanic stratigraphic model by integrating seismic and well-logs analysis and study the application of sequential indicator simulation that is based on local variation function in volcanic lithology simulation. First, a long-time isochronous stratigraphic structure is established by using conventional 3D seismic data, and then a high-precision volcanic stratigraphic framework is set up by multiwell correlation within the stratigraphic structure provided by conventional 3D seismic data. Another important aspect is the combination of sequential indicator simulation and local anisotropy joint simulation. Through seismic attribute analysis, the information of subsurface local anisotropy is deduced directly from the observed seismic data and converted into a local variation function model. The spatial distribution of lithology and physical properties of volcanic rocks is simulated based on facies control. (The lithology is different among different lithofacies, but it is similar in the same lithofacies.)

Geologic background

Shahejie Formation (Es) is a Paleogene stratigraphic unit of Bohai Bay Basin, China, which can be divided into four members: a fourth member of the Shahejie Formation (Es_4), the third member of the Shahejie Formation (Es_3), the second member of Shahejie Formation (Es_2), and the first member of Shahejie Formation (Es_1) from bottom to top. Large-scale lake transgression began in Es_3. Moreover, a set of dark gray mudstone intercalated with gray white and light-gray sandstone in Es_3.

Mudstone in the volcanic rock mass can be divided into two types: mudstone intercalation deposited in a short time during a volcanic eruption and mudstone barrier deposited during the volcanic dormant period. The discriminant criterion is whether it is stable between multiple wells (generally greater than 5 m). The mudstone barrier (the product of the volcanic dormant period) is used to resolve the volcanic rock mass into several volcanic eruption periods. Mudstone (Figure 3b) intercalation deposited in the volcanic eruption period. Finally, mudstone and volcanic rocks in the whole volcanic rock mass can be reasonably distinguished in a volcanic high-precision stratigraphic structure.

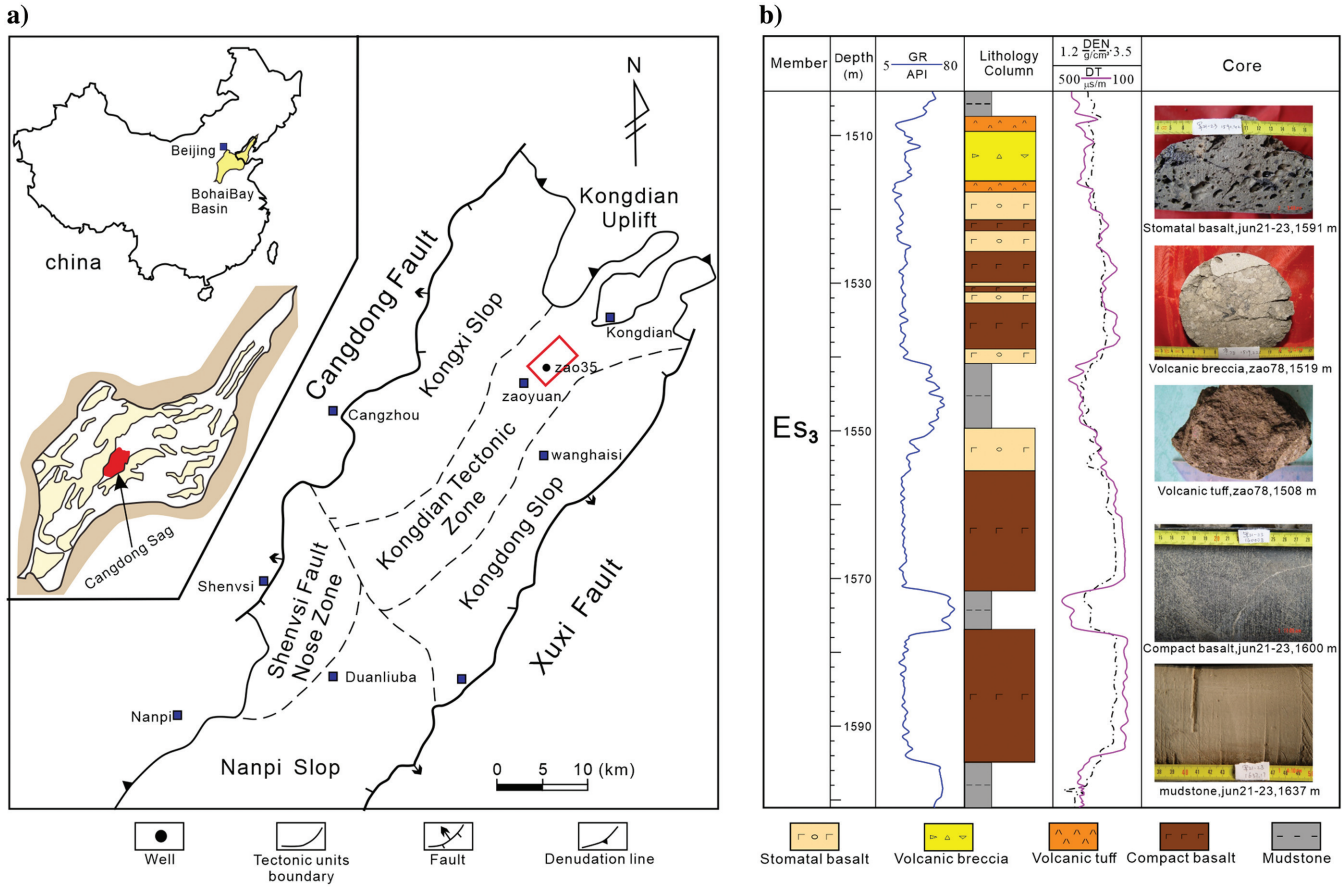

Figure 3. (a) Location of Zaoyuan oilfield and (b) well Zao35 lithology column and several core images of Es3 volcanic rocks. Zao35 block is located in the Kongdian tectonic zone of Cangdong sag in Huanghua depression, Bohai Bay Basin, China. Multiple large-scale volcanic activities formed multilayer extrusive rock. The extrusive rock mainly is stomatal basalt, compact basalt, volcanic breccia, and volcanic tuff.

DOI:10.1190/INT-2021-0048.1

Zao35 block is located in the downthrown side of Litianwu fault of Cangdong sag in Huanghua depression, Bohai Bay Basin, China (Figure 3a). The oil bearing is the third member of the Paleogene Shahejie Formation (Es_3), with a reservoir depth of 1505–1635 m (Wang et al., 2004). The lithology is a basic extrusive rock, and it is a kind of volcanic heavy oil reservoir with high porosity (average 15%) and high permeability (average 300 mD) (Zheng et al., 2006). A small faulted lake basin was developed in Es3, which was in an active period of volcanism. Multiple large-scale magmatic activities formed a multilayer volcanic rock mass (Figure 4). The lacustrine mudstone (Figure 3b) was deposited during the volcanic dormant period and is regarded as the interface between volcanic eruption periods.

Not all volcanic rocks can be reservoirs, and different lithofacies control the formation of different types of volcanic reservoirs. The distribution of volcanic rock mass is controlled by volcanic passage (Zhou and Zhang, 2010). It is essential to determine the relative relationship between volcanic conduits and volcanic rock mass and study the lithology and reservoir physical property changes within the volcanic rock mass (Wang et al., 2004). Zao35 block has three central volcanic conduits along the fault zone (Figure 5a), which is one large and two small sizes.

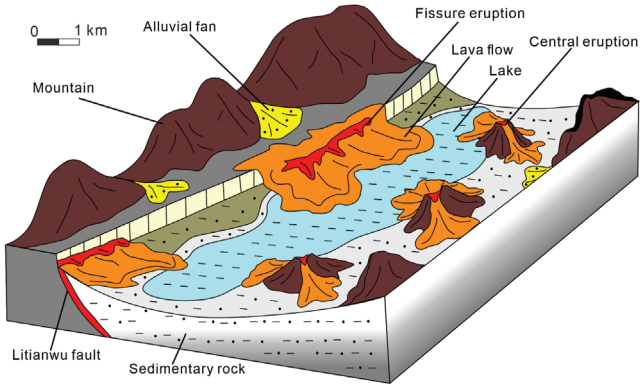

Figure 4. Volcanism model of Es3 member in the Zao35 block showing two eruption types and lava flow pushing into the lake in the downthrown side of Litianwu fault.

Methodology

In this paper, the volcanic activities are divided into three major stages based on conventional seismic data. Furthermore, the stages are divided into eight volcanic eruption periods by the relatively stable mudstone barrier (generally larger than 2 m) from the strata correlation of multiple wells. Controlled by seismic interpretation horizon and logging geologic stratification, the top and bottom surfaces of eight volcanic eruption periods were established. The trend changes of surfaces made up for the lack of wells. Finally, a 3D structural model with 15 zones (representing eight volcanic eruption periods and seven sedimentary rocks) was established.

The stochastic simulation method uses a global variogram model to represent the continuity pattern. It uses two-point geostatistics and variation function as a tool, but it cannot reflect the spatial correlation of more than

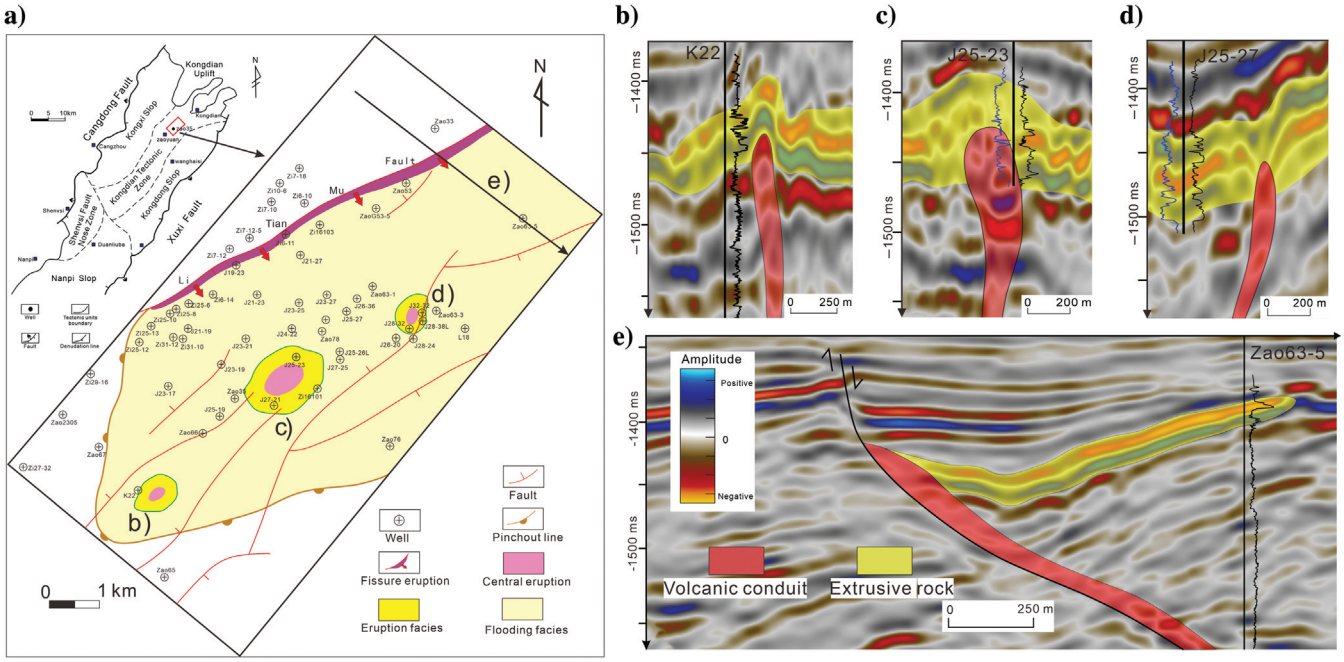

Figure 5. (a) Volcanic rock facies of Es3 member in the Zao35 block. The purple represents the location of the volcanic conduits, the deep yellow is eruption facies, and the light yellow is flooding facies. Flooding facies is widely distributed, whereas eruption facies are only near the central conduits. (b-d) Central erupting volcanic conduit and (e) fissured erupting volcanic conduit. The black lines are well trajectories with GR log in the left and the acoustic time log in the right. Central conduits exhibit the (b and c) coniform and (d) funnel shape.

DOI:10.1190/INT-2021-0048.1

two large points at the same time. Thus, the target form is difficult to recover (Deutsch and Journel, 1998). It is actually a lack of geologic model disclosure, so there is still room for improvement. Geostatistical modeling using local anisotropy is a hot topic in reservoir modeling and characterization, and worthy learning in the volcanic reservoir modeling. Based on the study of volcanic lithofacies distribution, the sequential indication simulation (SIS) of local variational function with variable range directions is used to reproduce the volcanism model in Zao 35 block. The lithology of four volcanic rocks is randomly simulated according to the lithofacies region. (Different volcanic rocks generally have different lithology.) The simulation results of the lithologic distribution model are more consistent with the shape of lava flow spreading around the crater. Then, 3D models of porosity, permeability, and fluid distribution were established by using the sequential Gaussian stochastic modeling in different lithologies. The model is fully consistent with logging data and closely combined with the analysis results of seismic data and volcanism models. It makes the model become more accurate.

Modeling technique

The key techniques and methods used in this paper are volcanic period modeling, facies control modeling, and SIS. In this paper, seismic amplitude data are used to divide volcanic stages. A positive-amplitude response indicates a volcanic stage, as well as a negative-amplitude response. Added well logs, the volcanic activities in each stage are further subdivided into more volcanic eruption periods through the seismic well tie. The key to the stage division of volcanic eruption periods lies in the determination of products at the volcanic dormant period. The common products of the volcanic dormant period are sedimentary rock (gray mudstone) in the Zao35 fault. Seismic scale division can only distinguish thick layer mudstone or multiperiod mudstone and volcanic rock lithologic combination, but it cannot respond to a single volcanic eruption period. Therefore, to analyze the internal structure of volcanic rock more precisely, the volcanic mass was further subdivided based on the well volcanic rock lithology data and the seismic period framework.

The facies control modeling is mainly based on: different volcanic rocks generally have different lithologies; and different lithology rocks generally have different properties, such as porosity, permeability, and so on. For instance, volcanic breccia of explosive facies has numerous pores, while compact basalt of overflow facies without pores. Stochastic simulation of lithology is carried out according to the lithofacies region. The physical properties were randomly simulated according to lithology regions.

Sequential indicator simulation is a stochastic simulation method based on indicator kriging estimation (Wang et al., 2010). In the studied area, the kriging estimation algorithm is used to calculate the estimate of the indicator variable, which gives an estimate of the probability distribution of the unknown position variable. Along the random path, the values in the cumulative probability distribution function are randomly selected as the internal interpolation. The newly simulated value is used as an indicator variable to recalculate the cumulative probability distribution function and get the simulated value of the next grid node in the random path. In the preceding process, the variation function gives an indication of the spatial correlation between variables. A great variety of geologic models are represented by different magnitude range directions and values.

Modeling

The purpose of volcanic reservoir modeling is to use geologic information comprehensively to accurately describe the reservoir characteristics of known well points and to predict the reservoir characteristics of nonwell areas. It mainly includes the distribution of lithology and the variation of physical property (Wang, 2015).

Taking Zao35 block as an example, a 3D geologic model of volcanic rock was established in four steps by using the idea of "period division" and "facies control modeling." The model indicates the internal structure analysis of volcanic rock mass. The 3D seismic tracing of volcanic rock mass was completed by combining well logs and seismic data, and a structural model of volcanic rock mass was established to reflect the profile of volcanic rock mass. Taking the seismic response inside the rock mass as the isochronous information time frame, the detailed comparison of volcanic eruption periods in a single well was completed, and the volcanic

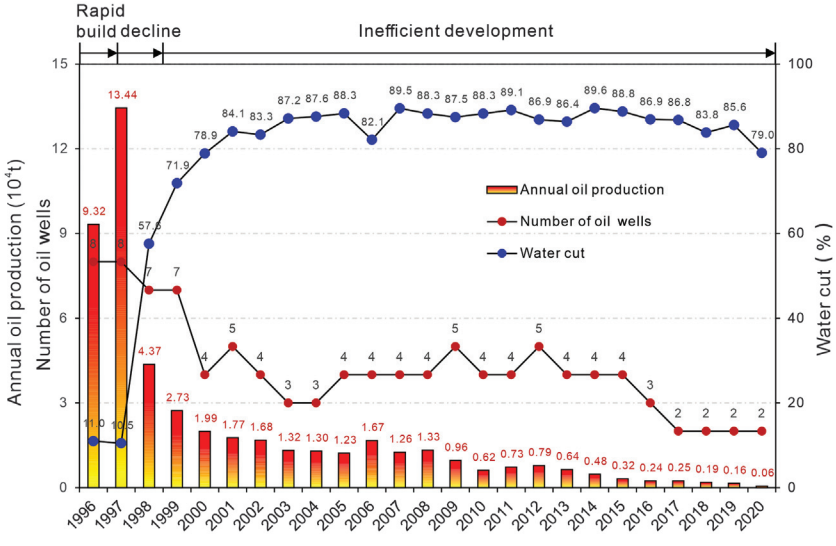

Figure 6. Development history of the Zao35 block indicating low development efficiency with a high-water-production rate of oil wells (90%) and a low annual oil production.

eruption periods in the rock mass were analyzed. The relatively stable mudstone was divided into the interlayers, and the thin mudstone was characterized as the interlayer. The stratigraphic structural model of volcanic rock mass was established by the method of period modeling. Based on the seismic response characteristics of volcanic conduits and volcanic facies, the volcanic eruption facies model and the volcanic facies model were established with volcanic eruption types. The physical property model is further completed through the combination of "phase-controlled" modeling ideas and sequential indication driver simulation.

Well data

As the volcanic reservoir is a special lithologic reservoir, the primary problem to be solved exactly lies in the lithologic development. Based on four coring wells (Jun 21–23, Zao78, Zao66, and Zao63-1) in the Zao35 block, five rock types can be found in this block: stomata basalt, compact basalt, volcanic breccia, tuff, and mudstone (Figure 3b). According to the porosity data of the volcanic rock core (Figure 17a), the porosity of volcanic rock has a close relationship to the lithology. The value of porosity is the largest in the pore basalt, followed by volcanic breccia and tuff. The compact basalt and mudstone are classified as nonporous states. The gamma-ray (GR) value of basic volcanic rocks is much lower than that of sedimentary rocks. Basalt without pores has a higher density. In addition, these five volcanic rocks and mudstone exhibit particular responses to distinguish in logging (Figure 7): Mudstone exhibits high GR value [greater than 60 American Petroleum Institute (API)] and high acoustic time (greater than 320 μs/m), compact basalt exhibits low GR value (less than 39 API) and low acoustic time (less than 250 μs/m), stomatal basalt exhibits low GR value (less than 47 API) and medium acoustic time (in the range of 250–355 μs/m), volcanic tuff exhibits low GR value (less than 45 API) and high acoustic time (greater than 300 μs/m), and volcanic breccia exhibits medium GR value (in the range of 45–58 API) and high acoustic time (greater than 320 μs/m). In view of the remaining 43 wells without coring, the lithology of this block is identified with the logging data. The standard well section of thick mudstone from the upper part of the third member of Shahe Formation was used to complete the standardization of logging curves. In total, 276 data of sample points in the core section of four coring wells were selected to establish multiparameter charts, such as GR versus sonic transit time (AC) intersections (Figure 7a), density (DEN) versus sonic transit time (AC) crossplot, compensated neutron (CN) versus AC crossplot, and GR versus CN crossplot. The truncation standard of each lithologic logging curve (Figure 7b) was picked up to complete the lithologic identification of 43 wells in this block, and the lithologic identification results had a high consistency with the coring data (Figure 7c).

According to the core observation and logging data of the coring well section, a large number of gray-brown and dark gray lacustrine mudstones have been developed in the volcanic rock mass, with a maximum thickness of up to 15 m. In addition, weathering crust logging response was not observed. The lacustrine mudstone was deposited during the volcanic eruption period and is regarded as the volcanic eruption period interface.

Porosity logging mainly uses the acoustic porosity calculated from acoustic logging data, which could reflect the matrix porosity of the rock (Dai et al., 1998). Permeability has a logarithmic relationship with porosity (Figure 17b). According to the relevant information, permeability logging interpretation is conducted based on the empirical relationship between matrix permeability and matrix porosity (Dai et al., 1998; Yang et al., 2016). The fluid saturation logging interpretation is obtained by combining deep and shallow resistivity logging with the saturation formula derived from the Archie formula. The rock electrical parameters are obtained through data analysis. By resetting lithology, the curves of porosity, permeability, and oil saturation (Figure 8b) are corrected to remove the impermeable layers of mudstone and compact basalt. Sample points from 43 wells (Figure 8a) were obtained for the next periods of geologic analysis and 3D geologic modeling.

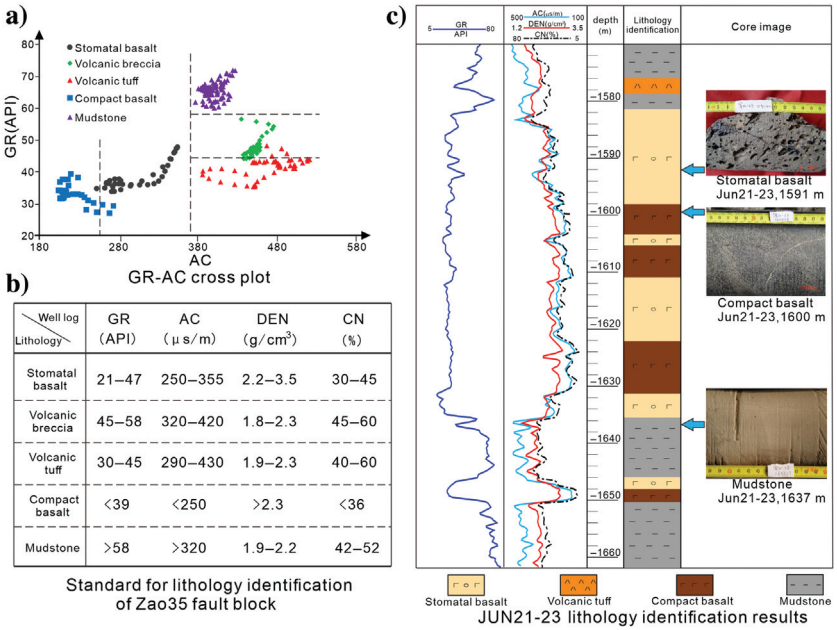

Well log / Lithology	GR (API)	AC (μs/m)	DEN (g/cm³)	CN (%)
Stomatal basalt	21–47	250–355	2.2–3.5	30–45
Volcanic breccia	45–58	320–420	1.8–2.3	45–60
Volcanic tuff	30–45	290–430	1.9–2.3	40–60
Compact basalt	<39	<250	>2.3	<36
Mudstone	>58	>320	1.9–2.2	42–52

Figure 7. (a) GR-DT crossplot and (b) standard for lithology identification of Zao35 fault block. Volcanic rocks are mainly less than 60 API in GR log, and in the range of 220–320 μs/m in the acoustic time log. (c) Jun21–23 lithology identification results. The core images indicate the well lithology identification result by logs.

DOI:10.1190/INT-2021-0048.1

All equations are as follows:

$$\Delta = \frac{\Delta t_{ma} - \Delta t}{\Delta t_{ma} - \Delta t_f}, \quad (1)$$

$$K = 0.0885 \times e^{\Phi}, \quad (2)$$

where Φ is the active porosity, decimal; Δt_{ma} is the acoustic time of rock skeleton, μs/m; Δt_f is the acoustic time of fluid, μs/m; Δt is the acoustic time, μs/m; and K is the permeability, μm^2.

Seismic data

The seismic data have undergone a 90° phase shift for a better match with the geologic body. The central frequency of seismic data volume is 20 Hz in the target depth, and a Rick wavelet with 20 Hz was the wavelet used (Figure 9). We use statistical methods to reliably estimate 30 wavelets from seismic (start time: −1350 ms and end time: −1600 ms) alone different well trajectory, and we average the wavelets to create a new wavelet, which can be substituted for a Rick wavelet with 20 Hz. Using the Rick wavelet (20 Hz), seismic synthetic records achieve the better matching relation and the balance of resolution and signal-to-noise ratio. Hence, the approximate mean wavelengths for the volcanic rock (4000 m/s, 20 Hz) and mudstone (2600 m/s, 20 Hz) were 200 and 130 m, respectively. In general, the maximum resolution of seismic data is only one quarter of the wavelength. The maximum resolution of volcanic rock is 50 m and the maximum resolution of mudstone is 33 m. Volcanic rock and mudstone have great differences in acoustic impedance (Figure 9), and the lithologic interface is a strong seismic reflection interface. Volcanic rock is mainly strong amplitude, and sedimentary rock has a weak amplitude.

Volcanic eruption is an abrupt geologic phenomenon of event. It is characterized by the variation of the eruption intensity and the diversity of the eruption center. Moreover, the sudden change of the thickness of the rock mass was common in a short distance. Volcanic rocks in different regions often present different characteristics. In the studied area with large well spacing, it is difficult to accurately track the top and bottom of volcanic rock mass by using wells information. Therefore, it is necessary to combine the 3D seismic data and make use of the seismic response difference between volcanic reservoir (Figure 10a, the yellow is an extrusive volcanic rock) and

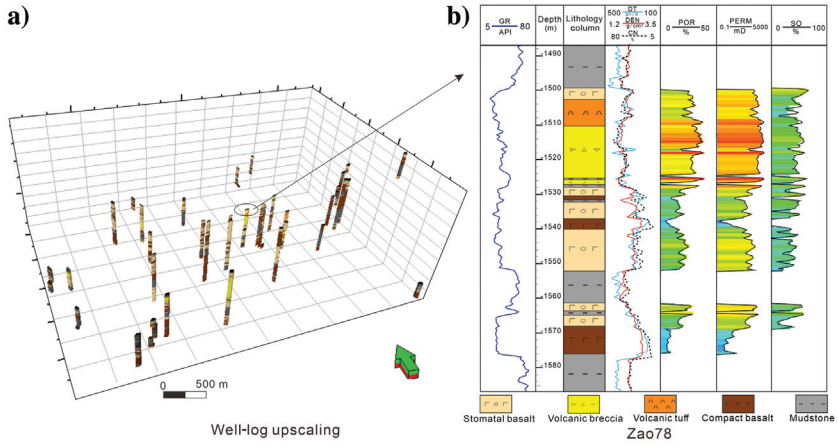

Figure 8. (a) Well-log upscaling and (b) Zao78 well. In the studied area, there are 47 wells samples with curves of lithology, porosity, permeability, and oil saturation that can be applied for 3D geologic modeling.

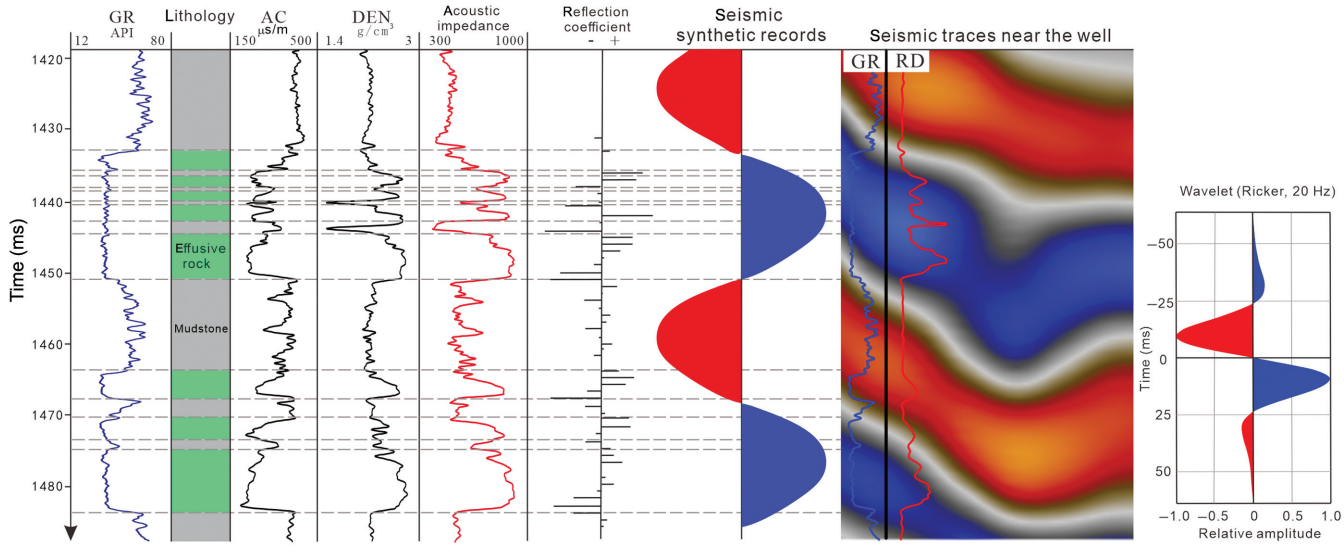

Figure 9. Seismic Synthetic records of Zao35 fault block (J 25–27). Volcanic rocks show characteristics of high impedance and high amplitude in the seismic synthetic record.

sedimentary rock to track volcanic body and the interpretation of top and bottom horizon of the body. According to the different seismic reflections between volcanic rocks and sedimentary rocks, the boundary of volcanic rock mass and the changes of the top and bottom surface can be determined by 3D seismic reflection tracing (Figure 10). Finally, taking the seismic interpretation horizon (time domain) as the trend, the top and bottom horizon of volcanic rock mass is established by using the well data (depth domain).

In the studied area, the type of volcanic eruptions is central eruption and fissure eruption. The central eruption has the shape of mound and dome seismic reflection, and it has the symmetry of the center. The seismic reflection shape of the volcanic conduit with central eruption is usually an umbrella and nearly upright column that diverges upward (Figure 5b–5d). Litianmu fault is a boundary fault of the Zao35 block, showing synsedimentary characteristics, and it also is a fissure magmatic conduit in the studied area. The deep and large fault of Litianmu communicated the lava chamber, and the basic lava upwelling along the fault formed a large area of the lava flow (Figure 5e). The volcanic rock mass is mainly characterized by overflow facies with good continuity in seismic amplitude, followed by depositional facies with medium to weak amplitude. Moreover, the explosive facies with poor continuity in seismic amplitude is confined to the area around the volcanic conduit.

Structural modeling

The key to the division of volcanic eruption periods lies in the determination of products at the volcanic dormant period. The common products of the volcanic dormant period are sedimentary rock (gray mudstone) in the Zao35 fault. The AC and radioactive logging (GR, U, and K) of sedimentary rocks and volcanic rocks are quite different from those of volcanic rocks. Volcanic rocks have low GR and low AC. Mudstone has high GR and high AC (Figure 7a). Through the information of coring and logging, the obvious discontinuous interface of volcanic eruption was identified in the vertical direction. In addition, the internal structure of volcanic rocks was analyzed by grade.

According to the well seismic calibration (Figure 9), the interior of the volcanic rock exhibits three periods of seismic response (Figure 10). According to the seismic amplitude response from bottom to top, stages I and III exhibit thick layers of basalt, and the stage II is characterized by thick mudstone, local basalt, and mudstone interbedding phenomena (Figure 11). The stage III is the most widely distributed, and it has the biggest thickness (75 m) in well J21–23.

Seismic scale division can only be distinguished from thick layer mudstone or multiperiod mudstone and volcanic rock lithologic combination, but it cannot respond to a single volcanic eruption period. Therefore, to analyze the internal structure of volcanic rock more precisely, the volcanic mass was further subdivided based on the well volcanic rock lithology data and the seismic period framework. Combined with the lithology data of 43 single wells, the restriction of three volcanic seismic periods, and the development of mudstone intercalation, the volcanic periods were further subdivided. Then, a 3D framework model (Figure 12) was established. Using seismic well tie, the volcanic activities in stage I can be subdivided into two volcanic eruption periods, one volcanic eruption period in stage II, and five volcanic eruptions periods in stage III, giving a total of eight volcanic eruptions.

Facies modeling

In this stage, the following models were developed: the volcanic facies model and the volcanic lithology

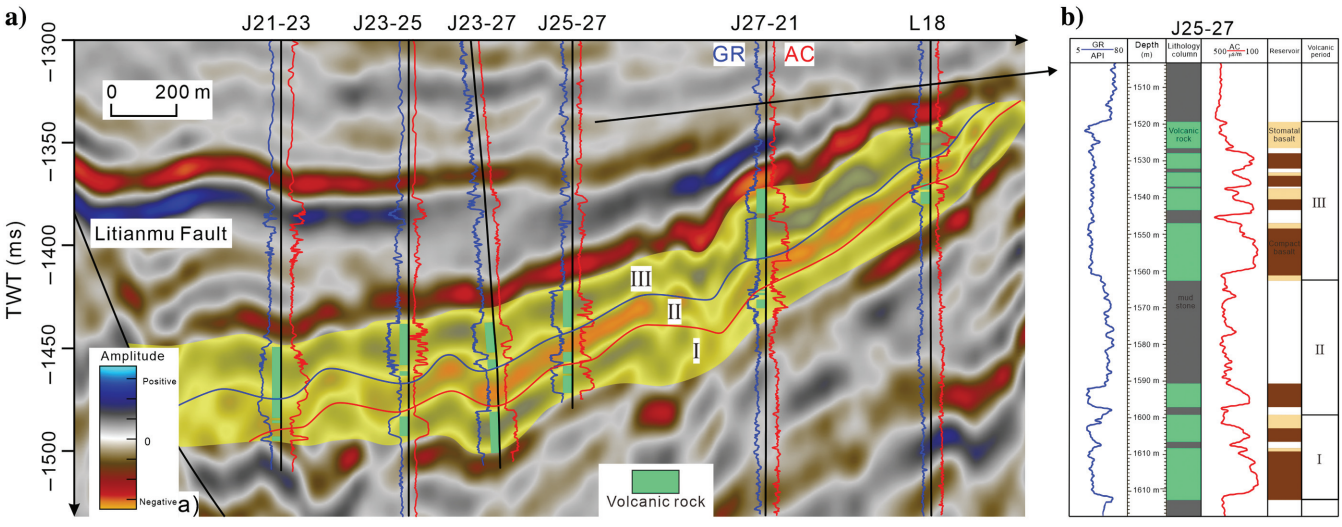

Figure 10. (a) Seismic section division of volcanic rocks in the Zao35 block and (b) division of volcanic rocks in J25–27. The interior of the volcanic rock exhibits three stages: two positive amplitude responses (stages I and III) and a negative amplitude response (stage II).

model. On the basis of identifying the seismic response characteristics of volcanic facies, a deterministic volcanic facies model was well established. Taking the lithologic development probability of different depths (Figure 16a) and the distribution of volcanic facies (Figure 16b) as the control, the sequential indicating modeling method with local variation function was adopted to establish a 3D geologic model of volcanic lithology (Figure 16c). When establishing the volcanic lithology model, the distribution of stomatal basalt, compact basalt, and mudstone interlayers was predicted in the overflow facies region. The stomatal basalt was the reservoirs, and the compact basalt was the nonreservoir. The volcanic breccia and tuff were predicted in the explosive facies region.

Volcanic facies mainly develop eruptive facies and overflow facies, and locally develop volcanic sedimentary facies and volcanic conduit facies. The volcanic conduit facies are mainly the fissure type and center type. The seismic reflection of the explosive facies has poor continuous and disorderly reflection characteristics (Figure 13a). The seismic reflection of the effusive facies has good continuous reflection characteristics and strong amplitude (Figure 13b). The volcanic conduits are characterized by poor continuity, and its seismic reflection structure shows a columnar, umbrella, and mushroom shape (Figure 5b–5e). The volcanic sedimentary facies is characterized by strong reflection from top to bottom, medium to weak reflection from inside, and medium continuity of seismic reflection. Volcanic facies (Figure 5a) were obtained by seismic attribute analysis (root-mean-square [rms] amplitude) combined with logging lithology. The volcanic facies model (Figure 16b) was established by a deterministic method (assigned by volcanic facies

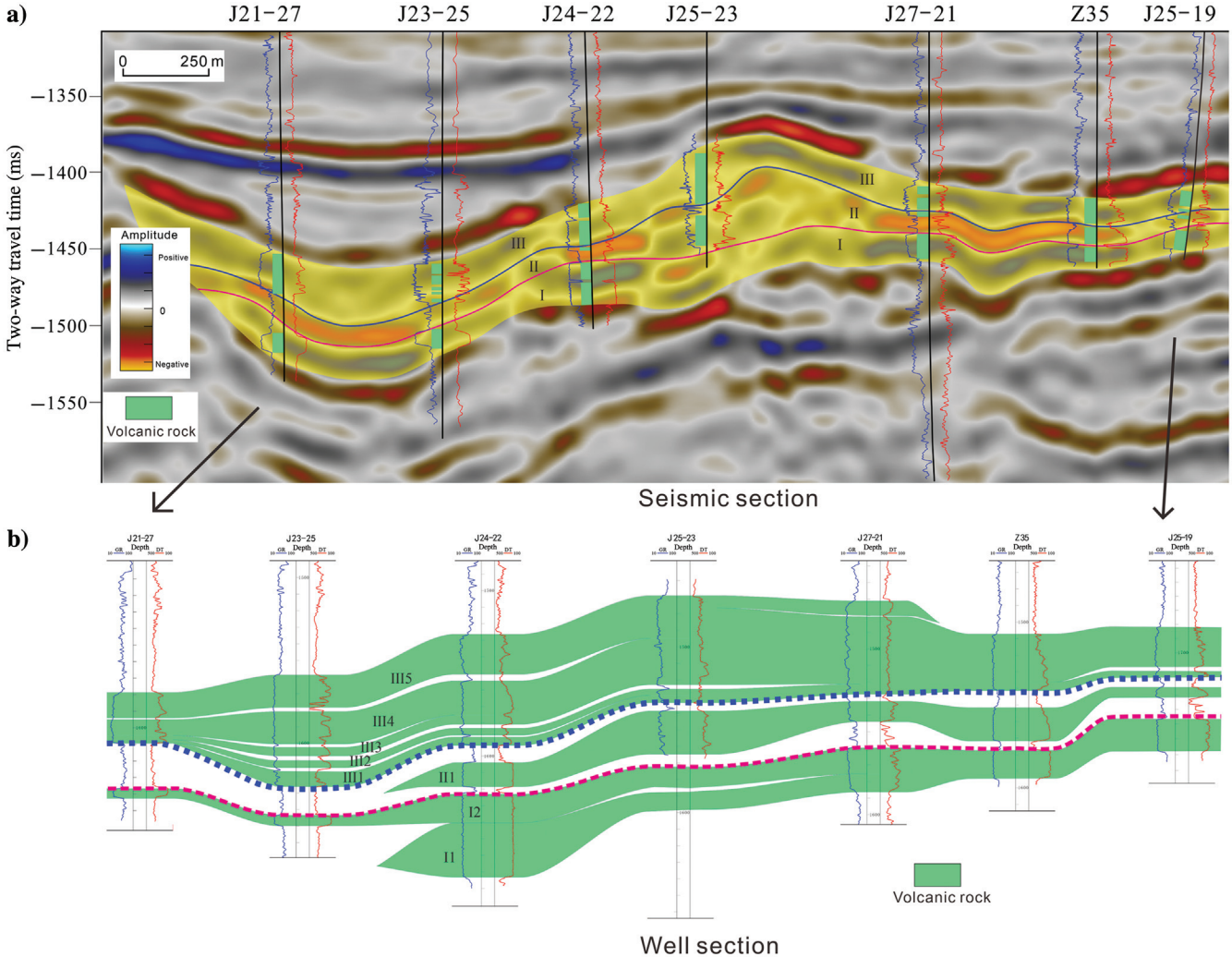

Figure 11. Division of volcanic eruption periods of Zao35 fault block: (a) seismic section and (b) well section. A section shows the result of volcanic eruption periods. According to well lithology column, the interior of the volcanic mass exists eight layers of volcanic rocks with seven layers of mudstone at most. The volcanic activities in each stage are further subdivided into more volcanic eruption periods: stage III has five volcanic eruption periods, stage II has one volcanic eruption period, and stage I has two volcanic eruption periods.

DOI:10.1190/INT-2021-0048.1

distribution map). The volcanic facies model is aimed to simulate the lithologic distribution by facies control.

The volcanic lithology can be realized by combining SIS with local variation function. The next paragraph mainly discusses how to establish local variable direction by volcanic eruption mode and obtain reasonable range value by seismic attribute when there is an insufficient number of wells.

Only 43 drilling wells cannot meet the needs of multidirectional variational function range analysis, so the rms amplitude information between the top and bottom layers of volcanic rocks is extracted (Figure 14a). Based on the previous studies on seismic properties of volcanic rocks in the Zao35 block (Zhou et al., 2014), it can be found of the seismic properties of amplitude. For instance, the maximum peak amplitude, total absolute amplitude, and total amplitude can better reflect the distribution range of volcanic rocks (Zhou et al., 2014). The rms amplitude was selected to identify the distribution of volcanic rock. This seismic attribute information (rms) has a good correlation (50%, Figure 14b) with the thickness of volcanic rocks, thus being able to approximately indicate the distribution of volcanic rock (Figure 14b) for variational function analysis in SIS.

The variogram direction refers to the direction with the best correlation between samples. The direction of the lava flow (extruded from volcanic conduit) is represented in the variogram direction. According to the

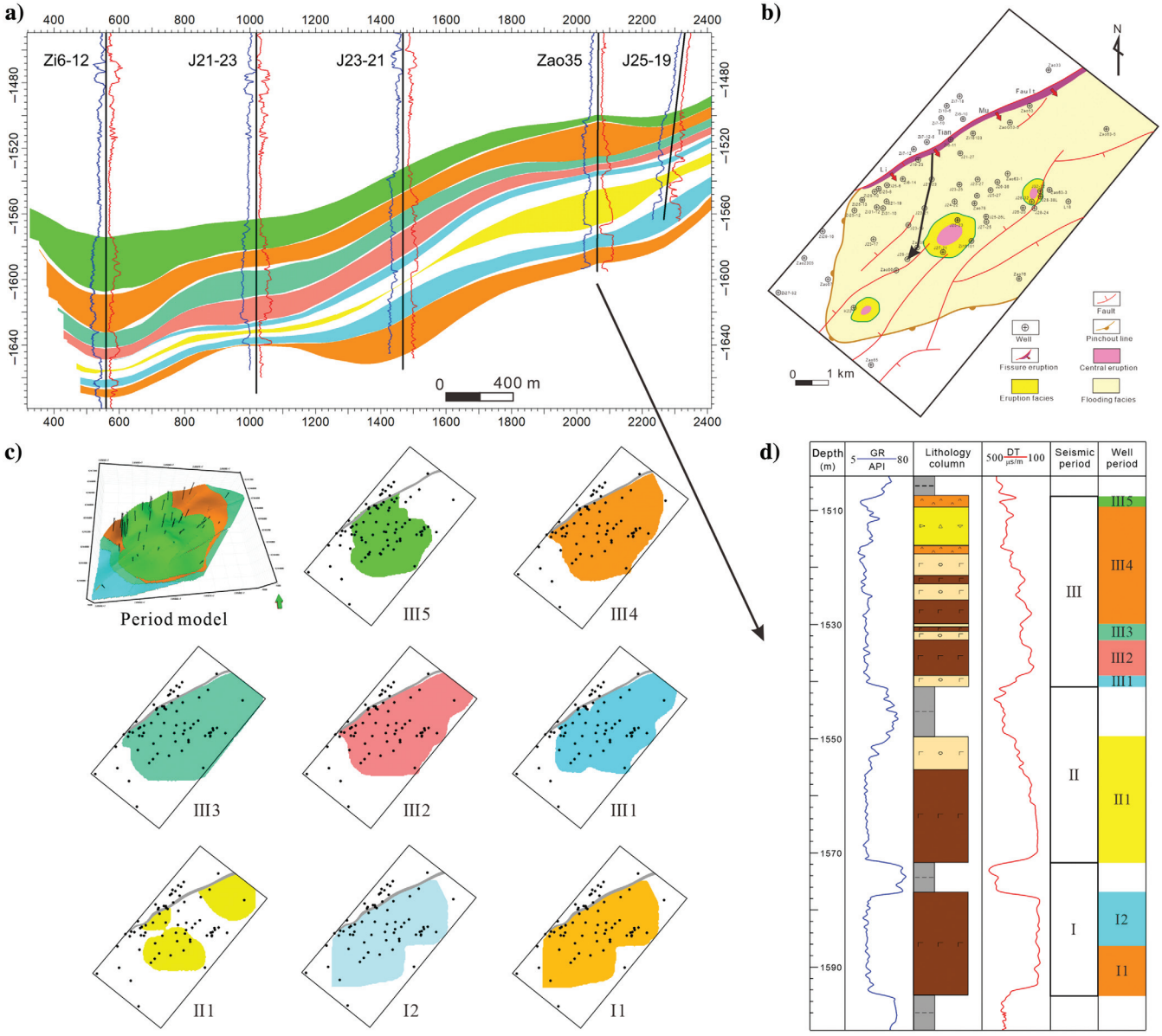

Figure 12. (a) Wells section of volcanic stage division in the Zao35 block, (b) location of the wells section, (c) volcanic periods division, and (d) division of volcanic rocks in Zao35. A section shows the thickness of each volcanic period. Stage III (III4 and III5) has the largest thickness; 2D plots show the distribution of each volcanic periods. Stage II1 has the smallest area. Volcanic activity gone through periods of intense active to relatively quiet to intense active.

DOI:10.1190/INT-2021-0048.1

volcanic facies distribution map, the studied area can be divided into different regions. The variogram direction of each region is in the direction of the lava flow. Three different types and their variogram direction are used to better express the ways. For a single flow with a fixed direction, the variogram direction is constant (Figure 15a). For a single flow with various directions, the variogram direction is different at each region (Figure 15b). Compared to the single flow, volcanism can be seen to have multiple lava flows from eruption centers. Therefore, the lava flow direction can be digitized in plane, and the lava flow direction can be represented by the numerical value of the variogram direction in different regions (Figure 15c).

The range of a variational function reflects the variable changes in a certain direction. Variables in the range are correlated, and variables out of the range are no longer spatially correlated. We choose the rms amplitude, which was selected to identify the distribution of volcanic rock. By fitting the experimental variation function at different directions (Figure 14c), the suitable maximum range value can be acquired by doing the corresponding analysis, which is 500 m in this studied area. The general of the main range is selected for the secondary range, which is 250 m. By setting the main direction and range of variation function, the volcanic eruption mode is applied to the random simulation of volcanic rock lithology and physical properties.

Property modeling

The evolution, composition, and structure of volcanic rocks, as well as the multistage tectonism and diagenetic stages experienced in the late period, succeed in making the volcanic reservoirs highly heterogeneous (Piao et al., 2016). Volcanic rocks of different lithologies show diversified physical characteristics. The porosity of stomatal basalt is the highest (average 22%), followed by volcanic breccia (average 17%) and volcanic tuff (average 12%) (Zheng et al., 2006), whereas the dense basalt has no effective pores (Figure 17a). The lithofacies model reveals a wide range of reservoir heterogeneity, and there are great differences in physical properties for different volcanic facies. Based on the lithology distribution, the physical property parameters are simulated to characterize the physical property heterogeneity of volcanic rocks. The stomatal basalt shows

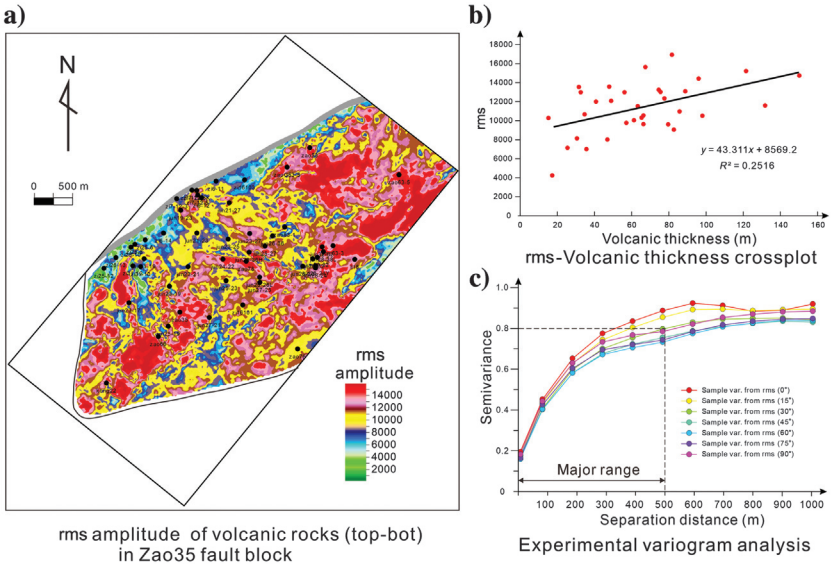

Figure 14. (a) The rms amplitude of volcanic rock (top-bot) in the Zao35 fault block, (b) rms-volcanic thickness crossplot, and (c) experimental variogram analysis. The rms has a good correlation (50%, b) with the thickness of volcanic rocks. The red in rms (a) indicates the areas of thick volcanic rock, whereas yellow indicates the areas of thin volcanic rock. The rms is used for variational function analysis to define the major range in SIS.

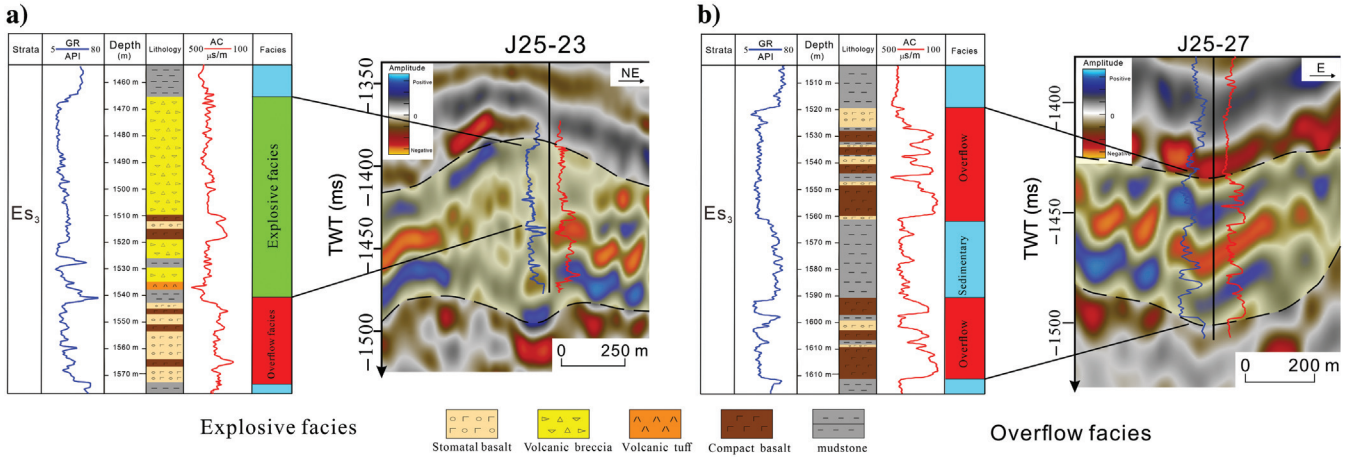

Figure 13. Volcanic facies and seismic reflection. (a) Explosive facies and (b) overflow facies. Explosive facies shows chaotic moderate amplitude seismic facies; overflow facies shows continuous high-amplitude seismic facies.

the best property, followed by volcanic breccia and tuff. The dense basalt has an interlayer of physical properties.

Under the control of the volcanic lithology model, sequential Gaussian stochastic simulation was carried out for different lithologies to obtain the porosity attribute model (Figure 17d). In the simulation of permeability in lithofacies, the porosity model was used as the collaborative data volume for sequential Gaussian stochastic simulation to obtain the permeability model (Figure 17e). When the oil saturation model is simulated, the porosity model is used as the collaborative data volume for sequential Gaussian stochastic simulation to obtain the oil saturation model (Figure 17f). A section (the black line in Figure 17c) exhibits the

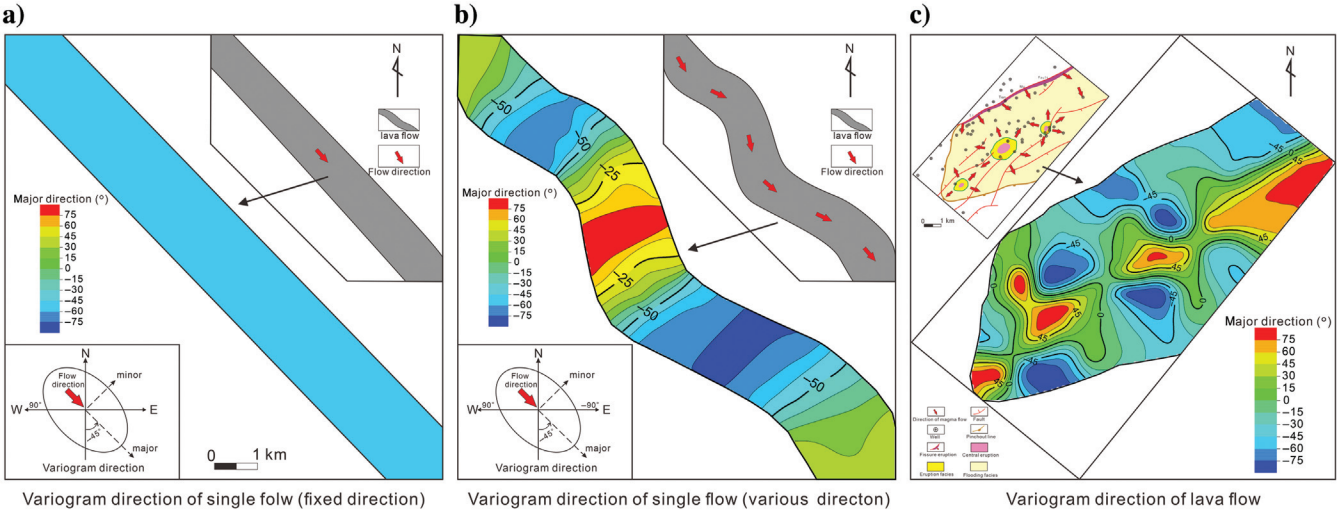

Figure 15. (a) The variogram direction of single flow (fixed direction), (b) the variogram direction of single flow (various direction), and (c) the variogram direction of the lava flow. For a single flow with a fixed direction, the variogram direction is constant (a). For a single flow with various directions, the variogram direction is different at each region (b). The lava flow direction can be digitized in plane, and the lava flow direction can be represented by the numerical value of the variogram direction in different regions (c).

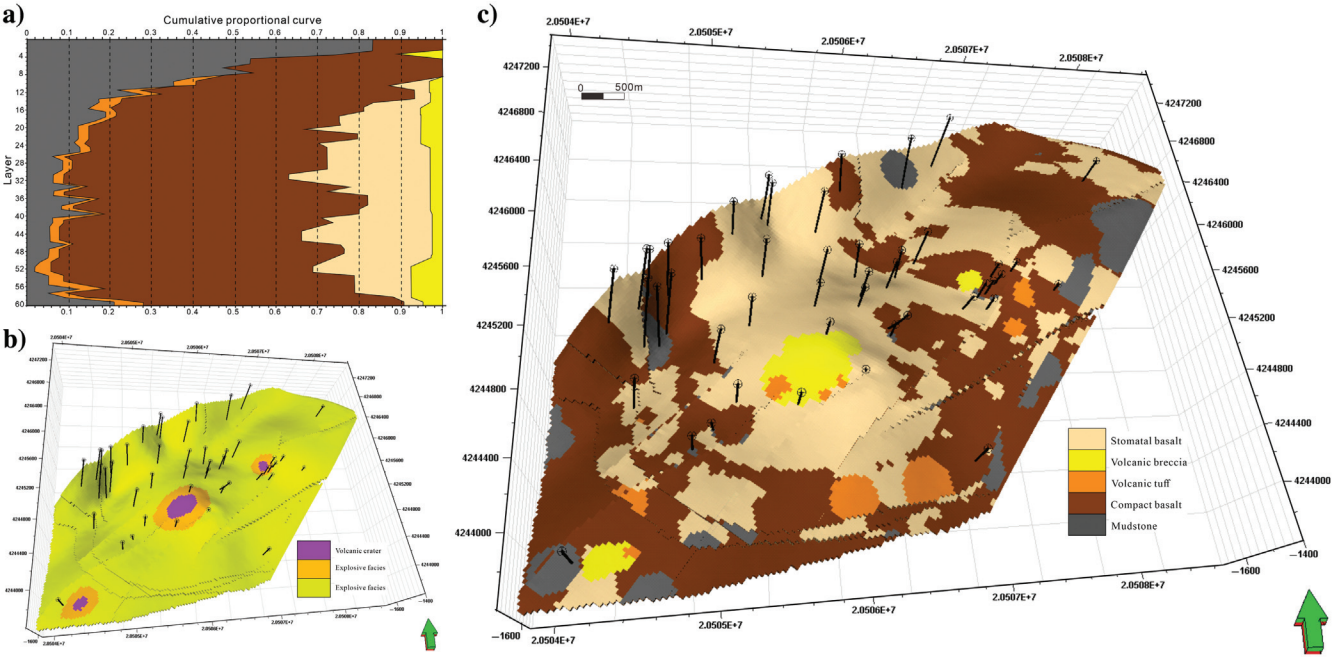

Figure 16. (a) Lithology cumulative proportional curve in different layers, (b) facies model of volcanic rocks in the Zao35 block; (c) lithologic model of Zao35 block in a 3D view. The statistical lithologic ratio of different depths can guide the simulation result in different depths. In the facies model, the overflow facies occupy more than 85% of the area, and the distribution area of compact basalt and stomatal basalt is the largest in the lithologic model. It also can be seen that stomatal basalt is mainly distributed near the volcanic conduit.

DOI:10.1190/INT-2021-0048.1

distribution of property (porosity, permeability, and oil saturation in Figure 17g–17i). Cool colors indicate the distribution of low value: blue in porosity and oil saturation; purple in permeability. The good reservoirs (por > 20%, perm > 200 mD, and So > 50%) mainly distribute in stage III (particularly, III5 and III4), and stage I has a small area of good reservoirs near well J23-21.

Model testing

Reservoir numerical simulation is conducted to study the physical properties of reservoirs and the flow laws of fluids by establishing mathematical models. Combined with the production dynamic data of the block, the reservoir history can be fitted, and the reliability of the 3D geologic model can be judged by the fitting accuracy (Chen et al., 2012). Experimental analysis of fluid parameters has existed in the studied area. The grid model can be obtained from the previous workflow. With special attention paid to the fact, the permeability parameter is the equivalent sum of matrix and fracture permeability. Zao35 fault block has 11 wells with production data, which were producing more oil in the early and then turned to inject water. Oil production and water production were simulated with the fixed liquid method, presenting a high overall fitting degree (Figure 18). The fitting degree of 11 oil wells is greater than 90%, all of which are characterized by high initial production and rapid decline.

Discussion

In the paper, the below contents would be specified It presents a high-precision stratigraphic structure modeling of volcanic rocks, and under the control of lithofacies, the volcanic rock lithology model is established

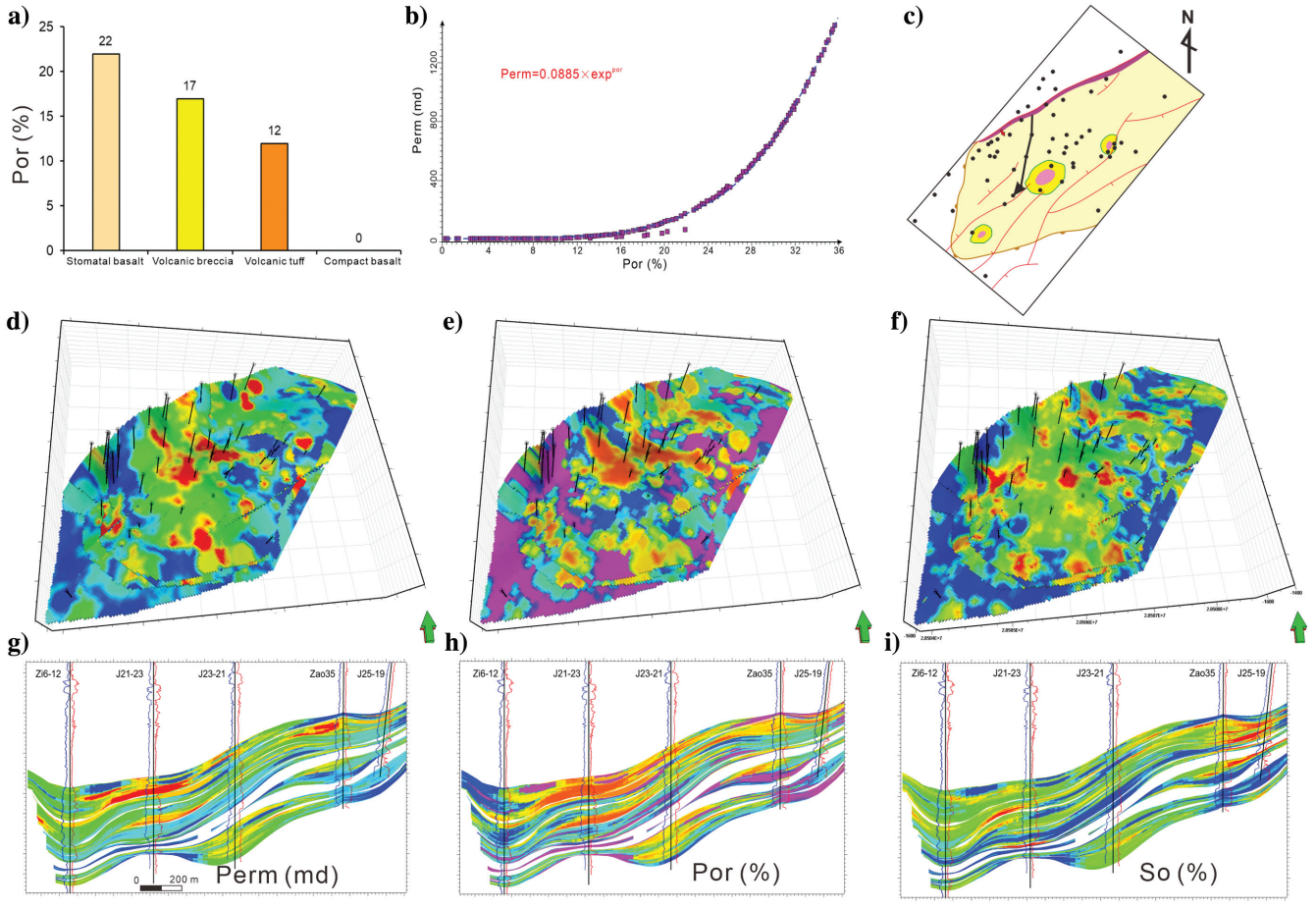

Figure 17. (a) Porosity in different lithology, (b) porosity-permeability crossplot, (c) location of the wells section, (d) porosity model, (e) permeability model, (f) oil saturation model, (g) porosity section, (h) permeability section, and (i) oil saturation section. The porosity of volcanic rock has a close relationship to the lithology, and the value of porosity is the largest in the pore basalt, followed by volcanic breccia and tuff in (a). A porosity-permeability crossplot shows that permeability has a logarithmic relationship with porosity in (b). (b) Volcanic rock facies of Es3 members in the Zao35 block. The purple represents the location of the volcanic conduits, the deep yellow is eruption facies, and the light yellow is flooding facies. The black line indicates the location of the (g) porosity section, (h) permeability section, and (i) oil saturation section. (d-f) The property models (porosity, permeability, and oil saturation) in a 3D view. The black lines represent well trajectories (47 wells). The cool colors indicate the distribution of low value (blue in porosity and oil saturation; purple in permeability). The section (porosity, permeability, and oil saturation) clearly reflects the distribution of property in (g-i). The good reservoirs (por > 20%, perm > 200 mD, and So > 50%) mainly distribute in stage III (particularly, III5 and III4), and stage I has a small area of good reservoirs near well J23-21.

DOI:10.1190/INT-2021-0048.1

by combining the sequential indicator simulation of local anisotropy.

At present, volcanic rock modeling is still in its infancy. Many scholars only build the structure model with one zone representing the whole volcanic rock mass, while ignoring the anatomy of the complex structure in the volcanic rock mass. The random simulation algorithm is only used to simulate the rock lithology. Such geologic models can hardly reflect the temporal characteristics of volcanic eruptions. Therefore, the idea of building a 3D structure model is proposed according to the volcanic eruption period. The high-precision isochronous stratigraphic structure, which takes the product of a single eruption period (volcanic rock) as the minimum stratigraphic unit, is greatly beneficial to fully reflect the period characteristics of volcanism in the random simulation of lithology.

Stochastic simulation of lithology (facies control) is a common method of 3D lithologic model building. However, the volcanic eruption model has complex and changeable morphology, and the global variogram cannot be used to characterize the complex geologic model effectively. Therefore, the complex geometry and lithologic discontinuities of volcanism can be better reconstructed by combining stochastic (sequential indicator) simulations with local anisotropy using local variational functions in different directions.

Moreover, fracture plays an important role in volcanic reservoirs. Although it cannot provide considerable oil storage space, it indeed plays a key role in connecting pores to form seepage channels. In the volcanic reservoir of the Zao35 block, there are only fracture interpretation results of core observation and single-well imaging logging, and there is no research on 3D fracture distribution. It is a significant research direction to establish the fracture model of volcanic rock by scale (large fault, fault, fracture split, and microfracture).

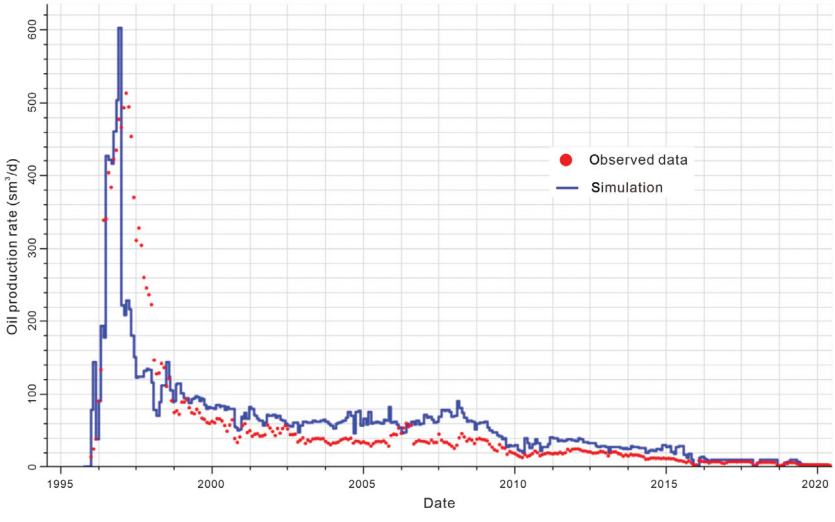

Figure 18. Simulation of oil production history in the entire Zao35 fault block. The blue line is the result of reservoir numerical simulation, and the red points represent the obverse data of oil production rate monthly. They have a high overall fitting degree.

Conclusion

This paper illustrates a workflow of establishing a high-precision volcanic stratigraphic structure model and reservoir properties model by integrating seismic data well data analysis. First, the seismic amplitude is used to define large-scale volcanic stages. Then, the large-scale volcanic activities are further subdivided into small-scale volcanic eruption periods by integrating the seismic and well data analysis. The seismic amplitude in our study area indicates that the interior of the volcanic rock exhibits three stages: two positive amplitude responses (stages I and III) and a negative amplitude response (stage II). Through the integration of seismic and well data in the studied area, as well as the seismic well-ties analysis, the volcanic activities in each stage are further subdivided into more volcanic eruption periods: stage III has five volcanic eruption periods, stage II has one, and stage I has two. A volcanic rock structure model with eight zones of volcanic rock and seven zones of mudstone barrier (15 zones in total) was established, which can effectively distinguish volcanic rocks (products of eruption period) from sedimentary rocks (products of the volcanic dormant period). The method of internal periods analysis and 3D modeling for volcanic reservoirs in the development stage is explored.

Based on the seismic-attribute analysis, the local anisotropy information is derived directly from the observed seismic data by combining the sequential indicator simulation and local anisotropy. The local anisotropy information is transformed into a local variation function model. The model of volcanism can be reproduced by SIS of local variogram with variable range direction, which exceeds the limitation of the complex volcanic eruption model that is difficult to be represented by the global variogram model. Based on the principle of facies control (lithology simulation is carried out in different regions according to lithofacies), the volcanic rock mass is simulated by the sequential indication method. The simulation results in better match the shape of lava flows spreading around the crater.

Acknowledgments

This work is supported by the National Natural Science Foundation of China (grant no. 42172154) and the Science Foundation of China University of Petroleum, Beijing (no. 2462020YXZZ022). We appreciate the geologists from the Dagang oilfield, CNPC for providing well and seismic data.

DOI:10.1190/INT-2021-0048.1

Data and materials availability

Data associated with this research are available and can be obtained by contacting the corresponding author.

References

Chen, B., Y. Xu, H. Yu, C. Liu, and L. Qu, 2012, Studies on uncertainty of 3D geological models of volcanic gas reservoir: Science Technology and Engineering, **12**, 4602–4606.

Chen, H., J. Yang, L. Wang, T. Li, Z. Ouyang, and L. Zhang, 2009, Volcanic eruption features of Laoheishan and Huoshaoshan in Wudalianchi: Global Geology, **28**, 291–296.

Cortez, M., and M. Cetalte-Santos, 2016, Seismic interpretation, attribute analysis, and illumination study for targets below volcanic-sedimentary succession, Santos Basin, offshore Brazil: Interpretation, **4**, no. 1, SB37–SB50, doi: 10.1190/INT-2015-0097.1.

Dai, S., X. Luo, J. Wang, and S. Jiang, 1998, Log response and interpretation of volcanic rock reservoir: Xinjiang Petroleum Geology, **19**, 3–5.

Deutsch, C., and A. Journel, 1998, GSLIB geostatistical software library and user's guide: Technimetrics, **40**.

Gamberi, F., 2001, Volcanic facies associations in a modern volcaniclastic apron (Lipari and Volcano offshore, Aeolian Island Arc): Bulletin of Volcanology, **63**, 264–273, doi: 10.1007/s004450100143.

Gao, Y., Y. Wu, W. Liu, X. Zhai, and H. Tang, 2013, Intercrystalline micropore characteristics and reservoir effect of Yingcheng Formation volcanic rock in Yingtai fault depression, southern Songliao Basin: Acta Petrolei Sinica, **34**, 667–674, doi: 10.7623/syxb201304006.

Gu, L., Z. Ren, and C. Wu, 2002, Hydrocarbon reservoirs in a trachyte porphyry intrusion in the Eastern depression of the Liaohe Basin, northeast China: AAPG Bulletin, **86**, 1821–1832, doi: 10.1306/61EEDD8C-173E-11D7-8645000102C1865D.

Hao, Q., J. Zhang, X. Li, W. Mao, and Y. Zhang, 2010, Seismic attribute oil-gas reservoir prediction technology and its application: Journal of Hubei University(Natural Science), **32**, 339–343.

Huang, Y., J. Shan, W. Bian, G. Gu, Y. Feng, B. Zhang, and P. Wang, 2014, Facies classification and reservoir significance of the Cenozoic intermediate and mafic igneous rocks in Liaohe Depression, East China: Petroleum Exploration and Development, **41**, 734–744, doi: 10.1016/S1876-3804(14)60087-2.

Infante-Paez, L., and K. J. Marfurt, 2017, Seismic expression and geomorphology of igneous bodies: A Taranaki Basin, New Zealand, case study: Interpretation, **5**, no. 3, SK121–SK140, doi: 10.1190/INT-2016-0244.1.

Jia, C., W. Zhao, C. Zou, Z. Feng, X. Yuan, Y. Chi, Z. Zhi, and S. Xue, 2007, Geological theory and exploration technology of lithostratigraphic reservoir: Petroleum Exploration and Development, **198**, 257–272.

Jiang, H., J. Guo, S. Guo, J. Luo, L. Jiang, and R. Qi, 2010, Present situation and prospect of exploration and development of igneous gas reservoirs in the world: Natural Gas Technology, **4**, 8–10.

Langella, A., D. Calcaterra, and P. Cappelletti, 2009, Lava stones from Neapolitan volcanic districts in the architecture of Campania region, Italy: Environmental Earth Sciences, **59**, 145–160, doi: 10.1007/s12665-009-0012-x.

Levin, L. E., 1995, Volcanogenic and volcaniclastic reservoir rocks in Mesozoic-Cenozoic island arcs: Examples from the Caucasus and the NW Pacific: Journal of Petroleum Geology, **18**, 267–288, doi: 10.1111/j.1747-5457.1995.tb00906.x.

Li, C., J. Chen, J. You, D. Wang, and J. Zheng, 2000, Study on volcanic reservoir modeling: Earth Science Frontiers, **7**, 381–389.

Li, S., C. Zhang, Y. Yin, T. Yin, and S. Yan, 2008, Stochastic modeling of reservoir with multi-source: Earth Science Frontiers, **15**, 196–201, doi: 10.1016/S1872-5791(08)60022-6.

Luo, J., Z. Qu, W. Sun, and F. Shi, 1996, The relations between lithofacies, reservoir lithology and oil and gas of volcanic rocks in Fenghuadian area: Acta Petrolei Sinica, **17**, 32–39.

Ogilvie, J. S., 2001, Characterization of volcanic units using detailed velocity analysis in the Atlantic Margin, West of Shetlands, United Kingdom: The Leading Edge, **20**, 34–50, doi: 10.1190/1.1438874.

Piao, Y., C. Liu, J. Zhu, and Y. Hua, 2016, Characteristics of volcanic development and hydrocarbon accumulation in Shuanglong area of Lishu fault depression: World Geology, **35**, 480–486.

Pike, R. J., 1978, Volcanoes on the inner planets — Some preliminary comparisons of gross topography: Lunar and Planetar Science Conference, **9**, 3239–3273

Qiu, P., L. Kong, D. Li, H. Su, X. Xia, and C. Zhou, 2017, Prediction of net pay zones in volcanic reservoirs with inner structures based on rock-mass controlled modeling: A case study of volcanic gas reservoirs in the Wucaiwan Sag, Junggar Basin: Natural Gas Industry, **37**, 48–55, doi: 10.3787/j.issn.1000-0976.2017.03.006.

Schutte, S. R., 2003, Occurrences of hydrocarbons in and around igneous rocks: Geological Society, Special Publication, **214**, 35–68.

Tang, H., and J. Pu, 2020, Review of volcanic reservoir geology: Acta Petrolei Sinica, **41**, 1744–1773, doi: 10.7623/syxb202012026.

Vernik, L., 1990, A new type of reservoir rock in volcaniclastic sequence: AAPG Bulletin, **6**, 830–836, doi: 10.1306/0C9B23A3-1710-11D7-8645000102C1865D.

Wang, F., 2015, Reservoir description and modeling of volcanic reservoir: Groundwater, **37**, 214–216.

Wang, H., Q. Ran, and Y. Hu, 2004, Lithofacies of igneous rocks in Dagang Zaoyuan oilfield: Petroleum Exploration and Development, **31**, 21–24.

Wang, P., G. Zhang, Q. Meng, B. Lu, D. Zhu, and X. Sun, 2011, Applications of seismic volcano stratigraphy to the vol-

canic rifted basins of China: Chinese Journal of Geophysics, **54**, 597–610, doi: 10.3969/j.issn.0001-5733.2011.02.039.
Wang, Y., J. Zhang, M. Wang, B. Pan, Y. Xin, and D. Shi, 2010, Simulation of lithology and porosity of volcanic rock reservoir based on sequential indicator simulation: Journal of Jilin University(Earth Science Edition), **40**, 455–460.
Wang, Y., and R. Zhang, 2012, Formation and distribution of volcanic oil and gas reservoirs in sedimentary basins of China: Science and Technology Wind, **206**, 219.
Wu, X., H. Li, Y. Yin, Y. Zhu, Z. Xu, and R. Xiong, 2009, Application of facies-controlled stochastic modeling in heterogeneity study: Fault-Block Oil & Gas Field, **16**, 58–60.
Xia, H., X. Huang, S. Wang, and L. Jun, 2005, The reservoir characterization at the regional character constrain: Progress in Geophysics, **29**, 769–774.
Yan, C., H. Yu, F. Yu, and D. Wang, 1996, Pores development and reservoir properties of volcanic rocks in Jianghan Basin: Journal of Jianghan Petroleum Institute, **18**, 1–6.
Yang, K., W. Bian, Y. Cai, X. Zhou, S. Xu, and Z. Lu, 2016, Petrological characteristics and logging response of Paleogene basalts in the eastern sag of Liaohe Basin: World Geology, **35**, 235–243.
Yao, F., F. Huang, and J. Ji, 2007, Reservoir evaluation and development effects of volcanic reservoirs in Zao35 fault block: Natural Gas Industry, **166**, 41–43.
Zangmo, G. T., A. D Kagou, and D. G Nkouathio, 2016, The volcanic geo-heritage of the Mount Bamenda CALDERAS (Cameroon Line): Assessment for geo-touristic and geo-educational purposes: Geoheritage, **9**, 255–278, doi: 10.1007/s12371-016-0177-0.
Zhang, B., P. Wang, G. Zhang, X. Sun, B. Lu, and W. Ni, 2013, Cenozoic volcanic rocks in the Pearl River Mouth and Southeast Hainan Basins of South China Sea and their implications for petroleum geology: Petroleum Exploration and Development, **40**, 704–713, doi: 10.1016/S1876-3804(13)60095-6.
Zheng, Y., Y. Wang, and Q. Ran, 2006, Study on volcanic reservoir characteristics of Zao35 fault block: Acta Petrolei Sinica, **27**, 54–58.
Zhou, D., and X. Zhang, 2010, Analysis on relationship between igneous lithofacies types and oil and gas reservoir: Coal Technology, **29**, 127–129.
Zhou, T., L. Ji, C. Xie, and L. Du, 2014, Distribution prediction of volcanic rocks in Zao35 fault block based on seismic attribute analysis technology: Journal of Yangtze University (Natural Science Edition), **11**, 70–73.
Zhu, R., Z. Mao, H. Guo, and J. Wang, 2016, Volcanic oil and gas reservoir geology: Thinking and forecast: Lithologic Reservoirs, **22**, 7–13.

Biographies and photographs of the authors are not available.